Rangeland Ecology & Management 72 (2019) 846–857

Contents lists available at ScienceDirect

Rangeland Ecology & Management

journal homepage: http://www.elsevier.com/locate/rama

Simulating Rangeland Ecosystems with G-Range: Model Description and Evaluation at Global and Site Scales☆

Jason Sircely [a,*], Richard T. Conant [b,c], Randall B. Boone [b,c]

[a] CGIAR Research Program on Climate Change, Agriculture and Food Security, International Livestock Research Institute, Nairobi 00100, Kenya
[b] Natural Resource Ecology Laboratory, Colorado State University, Fort Collins, CO 80523-1499, USA
[c] Department of Ecosystem Science and Sustainability, Colorado State University, Fort Collins, CO 80523-1476, USA

ARTICLE INFO

Article history:
Received 13 June 2018
Received in revised form 20 February 2019
Accepted 10 March 2019

Key Words:
model description
net primary productivity
rangeland
simulation model
vegetation dynamics

ABSTRACT

Rangeland ecosystems and their roles in providing ecosystem services are vulnerable to changes in climate, CO_2 concentration, and management. These drivers forcing widespread changes in rangeland ecosystem processes and vegetation dynamics create two-way interactions and feedback loops between biogeochemistry and vegetation composition. To support spatial simulation and forecasting in the global rangelands, the G-Range global rangelands model couples biogeochemical submodels from the CENTURY soil organic matter model with dynamic populations' submodels for herbs, shrubs, and trees. Here is presented a model description for G-Range, including novel elements of G-Range and implementation of CENTURY code. An initial evaluation of G-Range at global and site scales follows. G-Range outputs for net primary productivity (NPP) and vegetation cover (herbs, shrubs, trees, bare ground) were evaluated against global MODIS layers at global and site scales, and aboveground and belowground NPP were compared with field data from globally distributed sites. Most model outputs evaluated were within the range of *a priori* benchmarks for tolerable absolute or relative error (two benchmarks per output, at two scales, for five outputs of NPP and vegetation cover). Trade-offs in model fit among variables, datasets, and scales indicated practical constraints on improving model fit with respect to the selected evaluation datasets, especially field NPP versus MODIS NPP. The relative effects of multiple drivers of rangeland vegetation change were the greatest sources of uncertainty in model outputs. G-Range is best suited to scenario analysis of large-scale and long-term impacts of climate, CO_2, and management on rangeland ecosystem processes and vegetation, as well as ecosystem services, such as production of forage and browse and carbon sequestration.

Introduction

Rangelands, extensively managed grazing lands with natural or semi-natural vegetation (Grice and Hodgkinson, 2002), cover more terrestrial surface than any other land use, including most of the drylands that comprise nearly 40% of global land (White et al., 2002). These ecosystems account for substantial portions of the global C, water, and nutrient cycles and deliver local and global environmental benefits in the forms of hydrological regulation and C storage, among others. Rangelands provide much of the forage for a livestock sector that supports the livelihoods of 1.3 billion people globally, > 75% of whom are income poor (GASL, 2014). Many rangeland and dryland production systems face multiple stressors, with climate change intensifying the effects of other strains (Reid et al., 2014) ,such as drought, rangeland fragmentation, increasing human populations and livestock densities, and land degradation. Rangelands around the world will likely experience vastly different climate and CO_2 impacts, varying from potentially catastrophic in some regions to beneficial in others (Boone et al., 2018). The effects of intertwining global change drivers on the structure, composition, and function of rangeland vegetation are difficult to disentangle (D'Odorico et al., 2013), as are the cascading effects on ecosystem services, human well-being, and the vulnerability of people and rangeland ecosystems to future shocks. Forecasting responses of rangeland ecosystems to global change scenarios can support strategies for mitigation of global CO_2 emissions and for climate adaptation in dryland production systems.

Ecosystem change in rangelands reflects joint outcomes of drivers that influence biogeochemical cycles or shift the composition of

☆ Funding was provided by the International Livestock Research Institute, Nairobi, Kenya and the CGIAR Research Program on Climate Change, Agriculture and Food Security (CCAFS), through European Commission Grant Agreement AGRICAB Ref. 282621. CCAFS is funded by the CGIAR Fund Council, European Union, and International Fund for Agricultural Development.

* Correspondence and current address: Jason Sircely, Sustainable Livestock Systems, International Livestock Research Institute, PO Box 30709, Nairobi 00100, Kenya, Tel. +254 20 422 3000.
E-mail address: j.sircely@cgiar.org (J. Sircely).

https://doi.org/10.1016/j.rama.2019.03.002

vegetation, often generating further feedbacks on ecosystem processes and vegetation (Anderies et al., 2002). Drivers that alter woody-grass balance can entail major shifts in rangeland ecosystem functioning (Hibbard et al., 2003), as well as the ecosystem services provided (firstly, forage vs. browse). In drier, disequilibrium rangelands (Von Wehrden et al., 2012), high spatial and temporal variability (Le Houérou et al., 1988) and rangeland management practices result in lagging or otherwise nonlinear outcomes (Reynolds et al., 2007) reflecting feedbacks among climate, vegetation, hydrology, and soils (Huxman et al., 2005). Both degradation and rehabilitation processes are conditional on both climate and management (Dardel et al., 2014), making lagging ecosystem changes difficult to predict.

Simulation tools are well suited to exploring possible future rangeland production systems under such unpredictability and conditionality, yet there are few pragmatic tools for investigating how climate change and other global change drivers will alter the structure and function of rangelands (Derner et al., 2012). Most global models capable of simulating biogeochemistry alongside vegetation dynamics (Sitch et al., 2008; Piao et al., 2013) have certain disadvantages in rangelands. Most notably, savanna vegetation and woody-grass balance is often poorly represented (or not at all), and an emphasis on mechanistic representation of vegetation interactions may be constrained by the difficulty of predicting changes in complex adaptive systems such as arid rangelands.

To address the challenge of modeling ecosystem change in rangelands globally, the G-Range model was developed by coupling mechanistic biogeochemical submodels with empirically trained plant populations submodels. The composition of vegetation in terms of herb, shrub, and tree cover and bare ground shifts in response to environmental (primarily climate and atmospheric CO_2) and management (primarily grazing/browsing and fire) drivers, enabling representation of complex and variable rangeland ecosystems, from savannas to semi-desert, that cover large areas of the globe. These climatic and management drivers are expected to force future shifts in woody-grass balance in most rangelands around the world (D'Odorico et al., 2013) —not only in savannas—and G-Range provides an alternative, more phenomenological approach to modeling vegetation dynamics.

Here and in the associated appendices are presented a description of G-Range model elements and implementation, including changes from its biogeochemical foundation, the CENTURY soil organic matter model (Parton et al., 1993, 1987). Finally, an initial evaluation of G-Range outputs based on site- and global-scale data is presented. The primary objective of evaluation was to assess whether G-Range is fit for its purpose, simulating the cycling of C, N, and water, and vegetation dynamics, in rangeland ecosystems globally.

Material and Methods

Purpose

The G-Range global rangelands model simulates biogeochemical processes and vegetation change in grasslands, drylands, and other extensively grazed ecosystems. The model seeks to capture the dynamics of primary production of forage and browse, decomposition, and the cycling of C, N, and water. G-Range furthermore emulates vegetation dynamics by representing changes in, and interactions among, populations of herbaceous and woody plants.

The ambition of G-Range is to simulate the global rangelands with a single executable process. The model needed to be simple enough for rapid global simulation, yet it also needed to capture interannual and intra-annual variation and directional shifts in essential ecosystem processes, as well as differences in ecosystem process rates and competition among major rangeland plant growth forms, especially in savannas and other systems with mixed cover of herbaceous and woody plants. Finally, G-Range needed to provide for scenario analysis, including changes in climatic conditions and rangeland management regimes. After considering a large number of range and pasture simulation models, the CENTURY model (Parton et al., 1993, 1987) was selected to serve as the biogeochemical foundation of G-Range (Boone et al., 2011), and a few elements drew inspiration from the related SAVANNA model (Coughenour, 1994). CENTURY is one of the models most commonly used for investigating rangeland ecosystems, especially for carbon cycle research in rangelands (NREL, 2012). However, no implementation of CENTURY coupled with dynamic vegetation existed previously to support forecasting of changes in biogeochemistry and vegetation structure in rangelands above the landscape scale. SAVANNA requires months of effort to parameterize a single new site, making global or even national scale application intractable.

In G-Range, as vegetation cover changes through time, the respective influences of herbaceous and woody plants on ecosystem processes shift in accordance with their spatial cover. The capacity of the model to simulate biogeochemical dynamics alongside vegetation change enables projection of future rangeland ecosystems in response to contrasting scenarios driven by climate, management, and atmospheric CO_2 concentration. G-Range is well suited to large-scale, long-term projections of rangeland ecosystem structure and function according to scenarios describing changes in climate and CO_2 (Boone et al., 2018) and management primarily in terms of fire and livestock grazing and browsing.

Model Entities

G-Range runs on a monthly time step in unprojected geographic grid cells and currently supports grid cell resolutions of 1°, 0.5°, 0.25°, 0.167°, 0.1°, and 0.083°, defaulting to 0.5°. The default spatial extent includes all rangelands globally, although simulations may focus on finer spatial extents (e.g., regions or countries) to reduce simulation time. Parameters are assigned uniformly within "landscape units," grid cells in areas of the globe considered homogenous in the ecological and management factors regulating biogeochemical and vegetation dynamics. Landscape units are defined as 15 biomes (Ramankutty and Foley, 1999), 14 of which contain rangelands. A rangeland mask is defined on the basis of Global Land Cover Characterization (GLCC) land cover types (USGS, 2008), yielding the active simulation surface (Fig. 1).

Grid cells are the central model entity in G-Range, which comprise multiple lower-level model entities in a hierarchical structure. Grid cells contain surface litter and soil layers, as well as "facets" representing different types of vegetation (Fig. 2). Vegetation facets indicate spatial cover of three plant growth forms or functional types—herbs, shrubs, and trees—that together occupy a spatially inexplicit 1-km^2 area (with bare ground in the remainder) that represents the larger grid cell. The 1-km^2 area was selected merely to reduce computation time, which would be much longer at grid cell scale. Vegetation facets produce biomass and influence the surface and soil layers in accordance with their respective ecosystem process rates and spatial cover. Grid cells have one surface layer (microbial biomass associated with decomposing aboveground litter) and four soil layers, with each soil layer 15 cm deep, for a total depth of 60 cm.

G-Range is spatially explicit at grid cell scale, with model inputs from spatial layers driving ecosystem processes and vegetation dynamics according to the location and rangeland type (biome) of the grid cell. Within grid cells, the model is spatially inexplicit and simulates vegetation facets without reference to location inside the grid cell.

Vegetation facets are composed of vegetation layers and plant parts that represent, respectively, overstory versus understory vegetation and within-plant allocation and tissue turnover. The herb facet (facet 1) has three vegetation layers, herbs (vegetation layer 1), herbs under shrubs (two), and herbs under trees (three). The shrub facet (facet 2) has two vegetation layers, shrubs (vegetation layer 4) and shrubs under trees (five), while the tree facet (facet 3) has a single vegetation layer, trees (vegetation layer 6). The herb facet has only two plant parts, leaves (plant part 1) and fine roots (two). The shrub and tree facets have three additional parts: fine branches (plant part 3), coarse branches (four), and coarse roots (five).

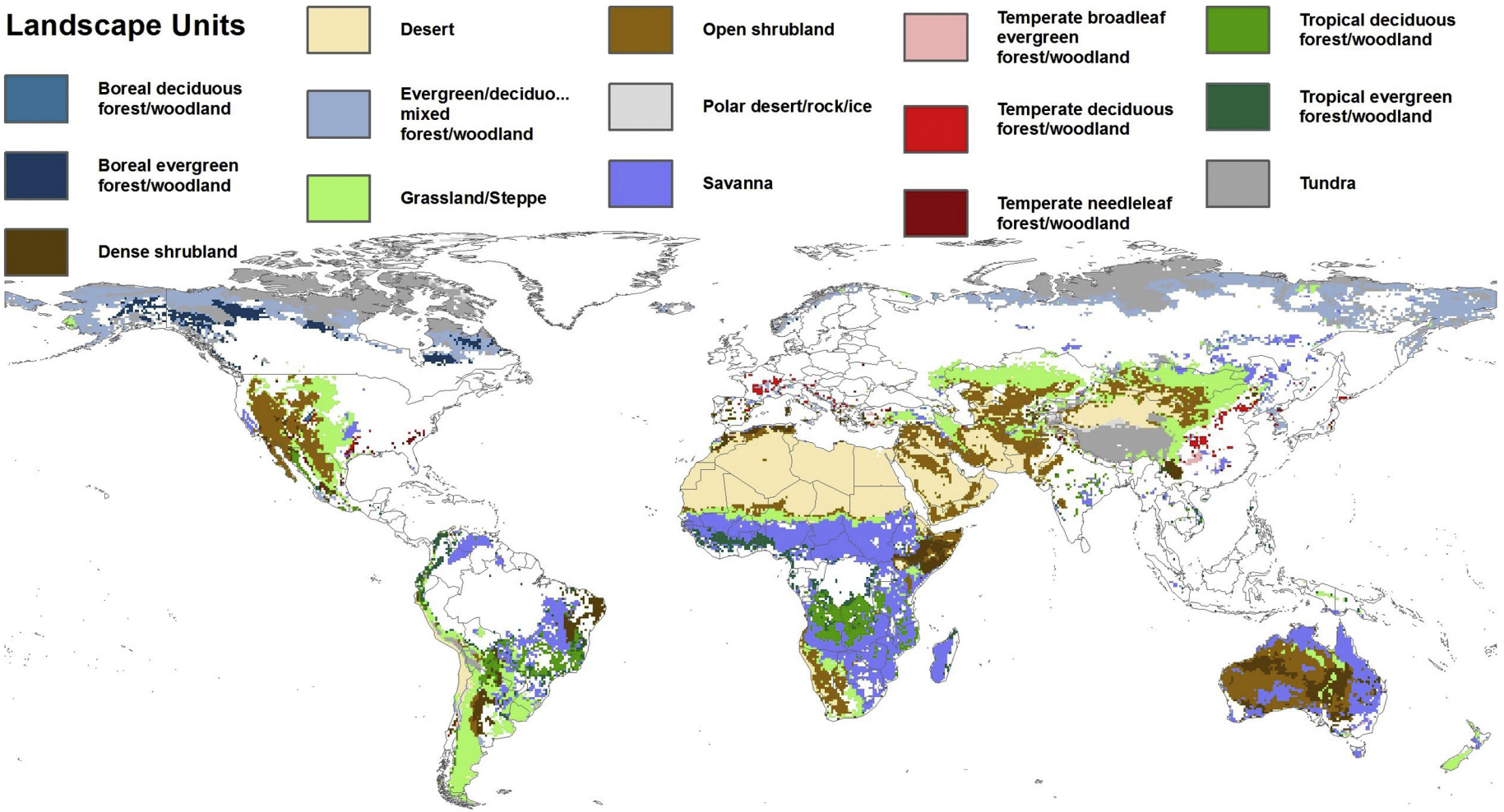

Figure 1. Active G-Range simulation surface. Parameter sets are divided among rangeland "landscape units" (i.e., biomes) (Ramankutty and Foley, 1999). Rangeland versus nonrangeland grid cells were defined on the basis of land cover types (USGS, 2008).

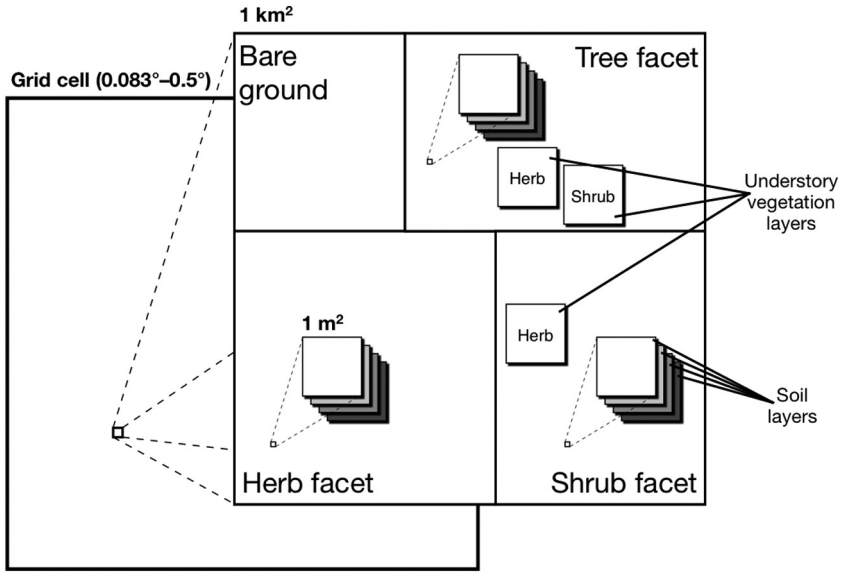

Figure 2. Conceptual diagram of central model entities within the hierarchical model structure of G-Range.

Vegetation facets are essential to the hierarchical structure of G-Range. Their most important role is to implement dynamics in vegetation cover. In addition, facet-level parameters, variables, and processes significantly but indirectly regulate biogeochemical dynamics at the grid cell level, through changes in the spatial cover of facets. Biogeochemical processes themselves—ranging from primary production and transpiration through effects of litter quantity and quality on decomposition and flows of C and N to soil pools—are simulated at the scale of 1 m^2 as in CENTURY and SAVANNA (CENTURY, which takes 1 m^2 as its central spatial unit, is actually point based or nonspatial; SAVANNA and G-Range nest these calculations into a hierarchical spatial framework). At the grid cell level, the magnitude of facet effects on biogeochemical processes scale with the spatial cover of the facet (see Fig. 2).

A large profile of model state variables captures variation in the attributes and dynamics of rangeland ecosystems and vegetation components, including ecological state variables and model parameters. Model state variables in G-Range fall into three main categories: 1) core state variables, 2) G-Range parameters, and 3) "hard-wired" parameters and variables, many originating from CENTURY (see Appendix A for full detail).

Core state variables (Appendix B) consist of a wide array of ecosystem attributes calculated from a 2000-yr "spin-up" simulation or a previous (post-spin-up) simulation. A spin-up is run to enable simulations to proceed from a long-term equilibrium. After a spin-up, core state variables are read from a saved state variable file at the beginning of a simulation. Saving a new state file at the end of a simulation allows for model inputs or parameterization to differ between time periods (e.g., to change climate or management).

Core state variables (Appendix B) and parameters (Appendix C) are variously assigned by grid cells, facets, vegetation layers, or plant parts. These two categories of state variables fall into several groups: "location" (geographic and climatic effects), "environmental" (environmental and abiotic effects and constraints), "management" (effects of management practices), "structural" (effects of gross ecosystem physical structure and plant community composition), "temporal" (timing of events), "functional" (ecosystem process rates), and "allometric" (effects of within-plant allocation and economics).

Model Design Concepts

The CENTURY soil organic matter model (Parton et al., 1993, 1987) has an established record as an ecosystem simulator for a variety of questions and purposes (NREL, 2012). CENTURY continues to be vetted and improved, and documentation is freely available (NREL, 2000). Development of G-Range began with adapting equations and model structures from CENTURY to accommodate spatial simulation of rangelands globally. Incorporation of the plant populations' submodels (Boone et al., 2011) drew some inspiration from the SAVANNA model (Coughenour, 1994). To optimize trade-offs among model complexity, applicability to scales and questions, availability of parameterization and input data, and programming and computation efficiency, CENTURY code was sometimes simplified or modified (for full detail, see Appendix A). A subset of parameters from CENTURY were "hard-wired" in G-Range (i.e., written into the Fortran 95 code compiled into the G-Range executable program), notably including pool-specific rates of soil organic matter turnover and associated respiration.

In G-Range, areal values for ecosystem stocks and fluxes of C, N, and water at grid cell level are primarily a function of the effects of vegetation facets on ecosystem processes and the respective cover of vegetation facets. Vegetation layers (within facets) incorporate effects of overstory competition on understory plant production, and plant parts (also within facets) represent the various biomass compartments of individual plants, their standing stock of elements, rates of growth, and rates at which dead plant materials of varying quality enter the litter and soil subsystems.

Decomposition is simulated as a cascading first-order decay model, where rates of decomposition are primarily controlled by assigning to each soil organic matter pool an intrinsic rate of decomposition and a fraction of C lost to respiration. Like CENTURY, G-Range has three soil organic matter (SOM) pools with different potential decomposition rates—fast (or active), intermediate (or slow), and passive—as well as aboveground and belowground litter pools and a surface microbial pool associated with decomposing aboveground litter. Although CENTURY maintains two separate multipliers used to modify decomposition rates due to 1) the combined effects of temperature and moisture *(defac)* and 2) the effect of anaerobic soil conditions *(anerob)*, G-Range combines all three effects into a single coefficient, as in SAVANNA. Fast SOM has two pools, surface (litter) and soil (0–60 cm), while intermediate and passive SOM each have a single soil pool (0–60 cm) and no surface pool.

The plant populations' submodels simulate the dynamics of plant populations and facet covers within a spatially inexplicit 1 km^2 area assumed to represent the larger grid cell. Plants establish and die in response to abiotic constraints and intrafacet and interfacet competition. Facet-level parameters specify potential linear effects of each factor on establishment or death, while conditions in the grid cell determine the

actual effects according to the parameterized linear relationships. Death is simulated before establishment each month, allowing repopulation of newly vacant areas. Bare ground within the 1-km^2 area is populated with new individuals of each facet, in this order: trees, shrubs, and herbs. Herbs and shrubs may establish in unoccupied understory areas beneath overstory shrubs or trees. The cover of the herb, shrub, and tree facets specifies the cover of the unshaded or overstory herb, shrub, and tree vegetation layers, while the cover of the overstory shrub or tree facet constrains the cover of the understory herb and shrub vegetation layers. Cover of bare ground is continually updated as the area not occupied by any facet.

Monthly plant death rates are calculated starting with initial, nominal death rates, parameterized at facet level. These nominal death rates are then additively modified by facet-specific parameters for linear effects of moisture stress, grazing intensity, and self-shading to obtain actual death rates:

$$d_i = n_i + w_g + g_g + c_g, \quad [1]$$

where n_i is the nominal death rate parameterized for facet i, w_g is the effect of moisture stress (as indicated by H_2O:PET, the ratio of available soil water to potential evapotranspiration) in grid cell g on the death rate, g_g is the effect of grazing intensity (fraction of live biomass removed), and c_g is the effect of self-shading (same-facet leaf area index; LAI). The product of the death rate d_i and total population of individual plants in each vegetation layer gives the number of plants dying in the current month. Because fire can potentially occur at any time of year, and only once per year (in G-Range), fire is handled separately from monthly mortality. When fire occurs, facet-level parameters for a linear relation between fire severity and the death rate give absolute plant mortality from fire, which is subtracted from the existing facet population.

Monthly plant establishment uses logic similar to plant death, with facet-level parameters setting initial, potential establishment rates, a dimensionless, relative value for propagule pressure. These potential rates are then modified by facet-specific parameters for linear effects of moisture stress, litter biomass, herbaceous root biomass, and woody overstory cover to obtain actual establishment rates:

$$e_i = s_i \times w_g \times l_g \times r_g \times c_g, \quad [2]$$

where s_i is the potential establishment rate parameterized for facet i, w_g is the effect of moisture stress (H_2O:PET) in grid cell g on the establishment rate, l_g is the effect of litter biomass, r_g is the effect of herbaceous root biomass, and c_g is the effect of overstory cover. Actual establishment, e_i, is constrained by existing plant cover. Woody and herbaceous plants have different competitive effects on establishment; shrub and tree cover indicate overstory competition, while herbaceous root biomass represents priority effects of prior habitat occupancy.

Biogeochemical dynamics, like CENTURY, are nonspatial yet calculated as though occurring at the scale of 1 m^2. However, because biomass production of understory herbs and shrubs is reduced by overstory competition, calculation of primary production is handled at the level of vegetation layers. The cover of the overstory shrub or tree facet serves as a proxy for the intensity of overstory competitive effects on understory production. In G-Range, ecosystem processes are simulated mechanistically using calculations functionally analogous to CENTURY, often using a code identical to CENTURY (generally CENTURY v4, and in some cases v4.5). The greatest difference between G-Range and CENTURY is that biogeochemical dynamics scale, according to dynamic vegetation cover, up to the level of individual grid cells distributed around the globe.

While the biogeochemical submodels operate independently from the plant populations submodels, the hierarchical structure of the model entails significant dependency among submodels. Areal, grid cell—level values of ecosystem fluxes involved in primary production, decomposition, and cycling of C, N, and water are almost entirely determined by process rates and facet covers:

$$p_g = \sum_{i=1}^{F} p_i \times c_i, \quad [3]$$

where p_g is the rate of a given ecosystem process in grid cell g, p_i is the rate of a given ecosystem process under vegetation facet i, c_i is the proportional cover of facet i, and F is the number of facets. The one exception to this rule is primary production of understory vegetation layers, which contribute additional production to their respective facets, as constrained by overstory shading. After calculation of primary production, attributes of the understory herb and shrub vegetation layers are recombined with their respective unshaded vegetation layers to obtain facet-level values for use in further computations.

In contrast to the mechanistic representation of biogeochemistry in G-Range, the controls over vegetation cover and dynamics are largely phenomenological in origin. In the plant populations' submodels, the wide variety of ecological factors affecting plant establishment and death are collapsed into a minimal set of primary effects on plant population growth and mortality. If these primary effects can reproduce observed vegetation structure in rangelands globally, they may sufficiently represent the full suite of factors thought to determine historical vegetation structure in rangelands around the world—notably climate, ecohydrology, fire, grazing, and plant competition. G-Range was trained to maintain a reasonable level of agreement with fractional vegetation cover from MODIS Vegetation Continuous Fields (VCF) (Hansen et al., 2006) over the course of a 2 000-yr simulation in which the past 100 yr of historical weather data (CRU, 2008) were looped repeatedly to generate a long-term dynamic equilibrium. That is, the primary objective in training the plant populations' submodels was to reproduce observed historical vegetation structure (from MODIS VCF) under historical climatic conditions over 2 000-yr simulations with qualitatively limited divergence.

The hierarchical structure of the model and inherent interdependency among the plant populations and biogeochemical submodels creates potential for a wide range of emergent ecosystem outcomes. Drivers such as climate and management can have several classes of direct effects on rangeland ecosystems in G-Range, by directly altering 1) ecosystem process rates only, 2) facet covers only, or 3) both ecosystem processes and facet covers. The effects of scenario drivers in G-Range differ among biomes and among individual grid cells in the same biome. When drivers such as climate and grazing alter ecosystem process rates while facet covers remain stable, ecosystem process rates at grid cell level will necessarily change (and may have feedbacks on future vegetation dynamics). The converse is also true—as facet covers change in response to the interplay among drivers and competition, so too will areal estimates of biogeochemical process rates, even if facet-specific rates remain unchanged. Drivers that directly affect ecosystem processes, as well as plant population dynamics, will influence both biogeochemical and vegetation dynamics at the same time, leading to emergent ecosystem structure and dynamics.

Grazing and fire are the primary management drivers in G-Range (even lightning-ignited fires are affected by land management via fuel loads). Fertilization is an option, though an uncommon practice in drier natural or native rangelands. Grazing and fire regulate biogeochemical processes directly, while more intense fire and grazing increase death rates, thereby influencing biogeochemistry indirectly as well.

Grazing affects biogeochemistry directly through effects on primary productivity and return of excreted nutrients. Grazing effects on productivity are similar to CENTURY—positive, negative, or neutral, depending on the response curve parameters selected and the intensity of grazing. G-Range takes the further step of using parameters to divide total "grazing" offtake (also a parameter) among the herb (grazing) and

shrub and tree facets (browsing) (see Appendix A). C and N in materials consumed by animals return to litter according to parameterized proportions.

Fire affects biogeochemistry directly by killing plant tissues and removing litter and standing dead biomass. Fire frequency defaults to parameterization, although fire frequency can be controlled by scheduling fire occurrence maps on a monthly or annual basis. Borrowing from SAVANNA, fire severity is a linear function of fuel load (total aboveground C) adjusted for flammability according to the proportion of live, green fuels (see Appendix A). When a fire occurs, parameters control the proportions of shoots, standing dead biomass, and litter that burn. The proportions of C and N in burned plant materials that are removed as volatile losses, versus deposited to litter in the form of ash, are also parameterized.

Intense grazing and fire influence population dynamics by exacerbating whole-plant death rates. Grazing effects on death rates are parameterized linear effects (see Eq. 1), as is fire mortality. Because fire can potentially occur at any time of year, and only once per year (in G-Range), fire mortality is calculated later in the subroutine, after the other effects on death rates (see Eq. 1), which are monthly and not annual. When fire occurs, the proportion of each facet killed by fire is a positive linear function of fire severity and newly dead individuals are subtracted from facet populations.

A few key assumptions implicit in G-Range, in addition to those inherited from CENTURY, can be significant considerations in interpreting model outputs (see also Appendix A). Woody plant cover (at grid cell scale) serves as a proxy for overstory competition, reducing the primary production and establishment of understory plants. Overstory effects on understory production use the CENTURY shading modifier, which assumes competitive suppression of the understory. The use of facet covers to represent overstory competitive effects on understory establishment invokes the simplifying assumption of more intense competitive effects on understory plants in areas favoring higher density and abundance of plant growth forms dominant in the overstory. This assumption is likely more valid at greater spatial and temporal scales and more likely valid in semiarid to humid rangelands than in truly arid rangelands.

The model furthermore assumes approximate functional equivalence at the facet level. That is, annual and perennial herbs, as well as deciduous and evergreen shrubs and trees, differ in terms of seasonal growth restrictions and subsequently differ in the timing of leaf death and deposition. Otherwise, general functional equivalence is assumed for individual plants within each facet. Key examples include productivity coefficients, tissue chemistry, and susceptibility to factors causing mortality, all of which are held identical for all plants in a facet.

Data

Initialization Data

Model initialization is conducted only if no "spin-up" simulation has been previously run to allow the model to proceed from equilibrium (e.g., 2 000 yr). Generally, a state variable file is saved from a spin-up and loaded into memory before proceeding with scenario simulations. To run a new spin-up, initialization is described in Appendix D.

Input Data

Historical weather data from the Climatic Research Unit (CRU) database (CRU, 2008) at 1° and 0.5° resolution for the yr 1901–2006 are currently included with model files available for download from the G-Range website (NREL, 2013). Weather data is stored in global (grid ASCII) maps, and is required to have the same resolution as the 'zone' (cell identifier) map. Monthly precipitation (cm) and monthly maximum and minimum temperature (°C) are read in at the beginning of each month.

The effects of a doubling in atmospheric CO_2 from 350 to 700 ppm on primary production of facets are read in from a scheduling parameter file, specifying modifying coefficients that increase the productivity of facets in response to rising CO_2 on an annual basis. Because the net effects of increasing atmospheric CO_2 on the productivity of various types of vegetation are not well characterized at large scales, coefficients representing net CO_2 effects can be increased or decreased to assess model sensitivity to putative effects of CO_2 on productivity and uncertainty in ecosystem responses to rising CO_2.

Fire and fertilization are incorporated in G-Range by default as parameters (Appendix C) specifying the frequency of fire and fertilization events probabilistically among cells and years and the proportional (within-cell) areal extent affected when a fire or fertilization event occurs. Alternatively, fire and fertilization can be scheduled using global maps specifying the proportions of each grid cell burned or fertilized on a monthly or annual basis. If the scheduling option is selected, maps specifying fire and fertilization are listed in scheduling parameter files and multiple maps can be listed to schedule shifts between management regimes throughout the course of a simulation.

Output Data

On a monthly basis, global surfaces for each layer of output variables are written to binary files (extension *.gof*) structured as a series of concatenated global maps for each layer of each output requested by the user. The number of layers possessed by an output variable is determined by the model entity to which it is assigned (i.e., one layer for grid cell — level variables, four layers for variables assigned by soil layers, three layers for facet-level variables, six layers for variables assigned by vegetation layers, and five layers for variables assigned by plant parts. An independent executable, the G-Range exporter, then subsets the binary files to produce a single monthly global gridded unprojected (geographic) ASCII map file for each layer of the output variable. The user then has the choice among any of a variety of platforms for processing and analyzing the global information system — friendly grid ASCII files.

Model Calibration and Evaluation

Model Calibration

Model parameters were subjected to a sensitivity analysis (Boone et al., 2013) and then modulated until a global-scale calibration was achieved in terms of model fit among a battery of global surfaces. Calibration sought agreement with global data layers centered on the yr 2006 or mean values for all years available and focused more intensively on novel G-Range parameters, especially those controlling vegetation dynamics in the plant populations' submodels.

Global layers used in calibration included CENTURY outputs (Henderson et al., 2015) for plant-available soil water, decomposition coefficients (*DEFAC*), soil organic C, annual net primary production (NPP), potential evapotranspiration (PET), and soil surface temperature. These layers were complemented by additional global layers for annual evapotranspiration (Zhang et al., 2010), snow-water equivalent (Armstrong et al., 2005), soil C:N (Batjes, 2002), Tier 1 live carbon density (Ruesch and Gibbs, 2008), and leaf area index (LAI) derived from ISLSCP II NDVI (Sietse, 2010). Calibration of vegetation cover sought to establish dynamic equilibria around 2000–2006 mean MODIS VCF (Hansen et al., 2006) fractional vegetation cover over the course of a 2 000-yr spin-up simulation using looped historical weather data from the 20th century (CRU, 2008).

Model Evaluation

As with other models that aim to simulate ecosystem dynamics and vegetation change at continental to global scales (e.g., Cramer et al., 2001), the performance of G-Range was judged on its ability to produce outputs that cut across clouds of data points from different locations and years. Simulation and forecasting of biomass production (i.e., forage and browse) is a central function of G-Range, and evaluation therefore focused on net primary production (NPP) and vegetation composition in

terms of herbaceous and woody cover. Evaluation of these model outputs would ideally use detailed, empirical data collected at the scale of globally distributed sites, complemented by global coverages derived from remote sensing. Because existing NPP databases at site and global scales each have their own advantages, limitations, and associated errors, NPP data from different sources and scales were selected to encompass more theoretically derived (MODIS) and empirical data (field measurements), obtained respectively at global and site scales. Following calibration, selective parameter adjustments were made to harmonize model fit with evaluation data at resolutions finer in terms of space (individual 0.5° grid cells) and time (multiple years of field data). Checks were performed to ensure that these parameter adjustments did not compromise the fit of the model to global-scale calibration datasets—including following repetition of the 2 000-yr spin-up simulation.

Evaluation focused on two spatial scales: 1) the global extents of focal biomes comprising major rangeland areas globally and 2) sites within these focal biomes with available field data. The four biomes fitting these criteria were "Tropical evergreen forest and woodland," "Savanna," "Grassland/steppe," and "Open shrubland" or semidesert (Ramankutty and Foley, 1999). Here, the term "biome" is used to describe these types rather than "landscape unit," the term in G-Range parameters and code.

Evaluation benchmarks in terms of absolute and percent differences between G-Range outputs and evaluation data (Table 1) were established to create criteria for evaluating cross-scale model performance. To obtain a model fit sufficient for global-scale application, it was determined that all G-Range output variables, at both global and site scales, should be on average within either the absolute or percent difference benchmark for a majority of the focal biomes. These a priori benchmark target ranges are somewhat arbitrary, and their values were set after quantitative and qualitative consideration of the magnitudes, scale-dependency, and uncertainty embodied in the various evaluation data sources available. A model able to produce simulation outputs within these ranges at both global and site scales should provide comparable or superior performance to other models currently available for long-term, dual simulation of global biogeochemistry and vegetation dynamics. If all model outputs analyzed had values within these benchmarks, it would not indicate perfect model performance. Rather, if all values were within benchmarks, it would indicate a parameterization striking a compromise in terms of model fit among multiple reference datasets from multiple sources across two scales of analysis.

Global, biome-level, total net primary production (TNPP = aboveground + belowground NPP) was evaluated against mean MODIS NPP (Zhao and Running, 2008) for the yr 2000–2006. G-Range TNPP was summed across all vegetation layers of all facets. Evaluation of TNPP against MODIS estimates used all 0.5° cells with MODIS TNPP > 0 in the focal biomes. Cells with MODIS TNPP = 0, which appeared unreliable in sparsely vegetated areas, were treated as missing values. Global facet cover was compared with 2000 − 2006 mean MODIS VCF herbaceous and tree cover (Hansen et al., 2006). Cover of the tree facet in G-Range was evaluated directly against MODIS tree VCF. Because MODIS herbaceous VCF aggregates cover of herbaceous and smaller woody plants, cover of the herb and shrub facets from G-Range were summed as herb/shrub cover and compared with MODIS herbaceous VCF. In addition to global contrasts, TNPP and facet cover were evaluated against the same global layers at grid cell level for sites with available field data.

At site scales, modeled herbaceous annual aboveground net primary production (ANPP) was evaluated against field measures of herbaceous ANPP estimated from biomass harvest ("field ANPP"), quantified as peak standing crop, the sum of annual maximum live and recent dead biomass (excluding litter). Belowground net primary production (BNPP) was evaluated against two measures of herbaceous annual BNPP: 1) BNPP field measures ("field BNPP") from root-ingrowth or minirhizotron methods in the few sites and years where available and otherwise from root biomass harvest; and 2) BNPP calculated from a standard global regression equation ("regression BNPP") as a function of field ANPP and mean annual temperature (MAT) (Gill et al., 2002). Regression BNPP, a method relying on turnover rates from sequential coring techniques known to be unreliable (Milchunas, 2009), is presented for purposes of comparison with field BNPP.

Field measures of BNPP from root biomass harvest were calculated as the MAT-weighted mean of two root production indicators providing, respectively, liberal and conservative estimates (Scurlock et al., 2002) of root production: 1) annual maximum root biomass and 2) annual maximum–minimum root biomass. Annual maximum root biomass often overestimates BNPP, especially in cold climates with slow turnover, while annual maximum–minimum root biomass often underestimates, especially in hot climates with rapid turnover. At the lowest MAT (−4.3°C) among the evaluation sites, maximum root biomass was weighted at 0, maximum–minimum root biomass was weighted at 1, and BNPP was calculated as the mean of the two weighted indicators. As MAT increased to the highest among sites (33.2°C), indicator weights increased linearly to 1 and 0, respectively (for full detail, see Appendix E).

Evaluation of ANPP and BNPP at site scales used data from all years with field data available. ANPP and BNPP data from plots with no woody overstory were compared with G-Range ANPP and BNPP for the unshaded vegetation layer of the herb facet. The final dataset

Table 1
Model evaluation benchmarks and results summary. For value presented in bold typeface, G-Range outputs did not meet evaluation benchmarks (for full evaluation results, see Appendix E, available online at https://doi.org/10.1016/j.rama.2019.03.002).

					Modeled–observed difference, by biome ("landscape unit")							
			Benchmarks		Tropical evergreen forest		Savanna		Grassland/steppe		Open shrubland (semidesert)	
Variable and units	Scale	Data source	Absolute difference (Abs.)	Percent difference (%)	Abs.	%	Abs.	%	Abs.	%	Abs.	%
TNPP	Global	MODIS NPP	300	100	141.0	34.7	99.3	**121.1**	−33.7	49.3	−47.3	16.1
($g\ C\ m^{-2}\ yr^{-1}$)	Site	MODIS NPP	300	100	**465.6**	95.9	155.2	**121.5**	−37.6	10.3	81.3	47.5
ANPP	Site	Field	100	100	**−103.5**	−29.7	−59.1	**107.0**	−17.5	59.0	26.6	**137.9**
($g\ C\ m^{-2}\ yr^{-1}$)												
BNPP	Site	Field	200	100	**−514.6**	−63.5	**−321.4**	30.5	−102.9	**246.5**	186.7	**974.0**
($g\ C\ m^{-2}\ yr^{-1}$)	Site	Regression	200	100	−42.1	−11.5	−63.0	−6.1	−148.1	-48.1	−159.0	−52.8
Herb/shrub cover	Global	MODIS VCF	25	100	11.0	28.8	12.3	22.7	9.1	**100.3**	42.8	**705.3**
(% cover)	Site	MODIS VCF	25	100	13.2	18.8	8.8	12.9	−16.0	−13.7	18.3	**100.9**
Tree cover	Global	MODIS VCF	25	100	−18.3	−10.2	−8.2	86.4	−1.4	**321.5**	2.3	**282.4**
(% cover)	Site	MODIS VCF	25	100	9.8	**193.9**	6.8	**226.4**	−0.1	**254.2**	0.0	0.0

TNPP indicates total net primary productivity; NPP, net primary productivity; ANPP indicates aboveground net primary productivity; BNPP, belowground net primary productivity.

comprised 317 site-yr for field ANPP (and regression BNPP) and 97 site-yr for field BNPP (Appendix E).

Results

Model Evaluation

Because G-Range is primarily designed for global application, evaluation results are reported for global coverages of the four rangeland biomes evaluated and among sites within those biomes. For full global and site-level evaluation results, or for regional or location-specific results and model errors, see Appendix E.

At both global and site scales, G-Range total net primary production (TNPP; aboveground + belowground) difference from MODIS TNPP was generally within the established a priori benchmarks for tolerable model error in terms of absolute and percent difference (see Table 1, Fig. 3, Fig. E.1). In savannas, G-Range exceeded the percent difference benchmark for TNPP at both global and site scales. Tropical evergreen forest ("tropical evergreen forest and woodland") exceeded the absolute difference benchmark at site but not global scales.

Difference in G-Range aboveground net primary production (ANPP) from field ANPP among all site-yr of available data was within the absolute difference benchmark for sites in savanna, open shrubland, and grassland (see Table 1, Fig. 4). Of these biomes, the percent difference benchmark was exceeded slightly in savannas and moderately in open shrubland. Tropical evergreen forest sites narrowly exceeded the absolute difference benchmark.

G-Range belowground net primary production (BNPP) was within benchmarks for percent difference, but not absolute difference, from field BNPP for sites in the two more productive biomes, tropical evergreen forest and savanna (see Table 1, see Fig. 4). In contrast, sites in the less productive biomes, grassland and open shrubland, were on

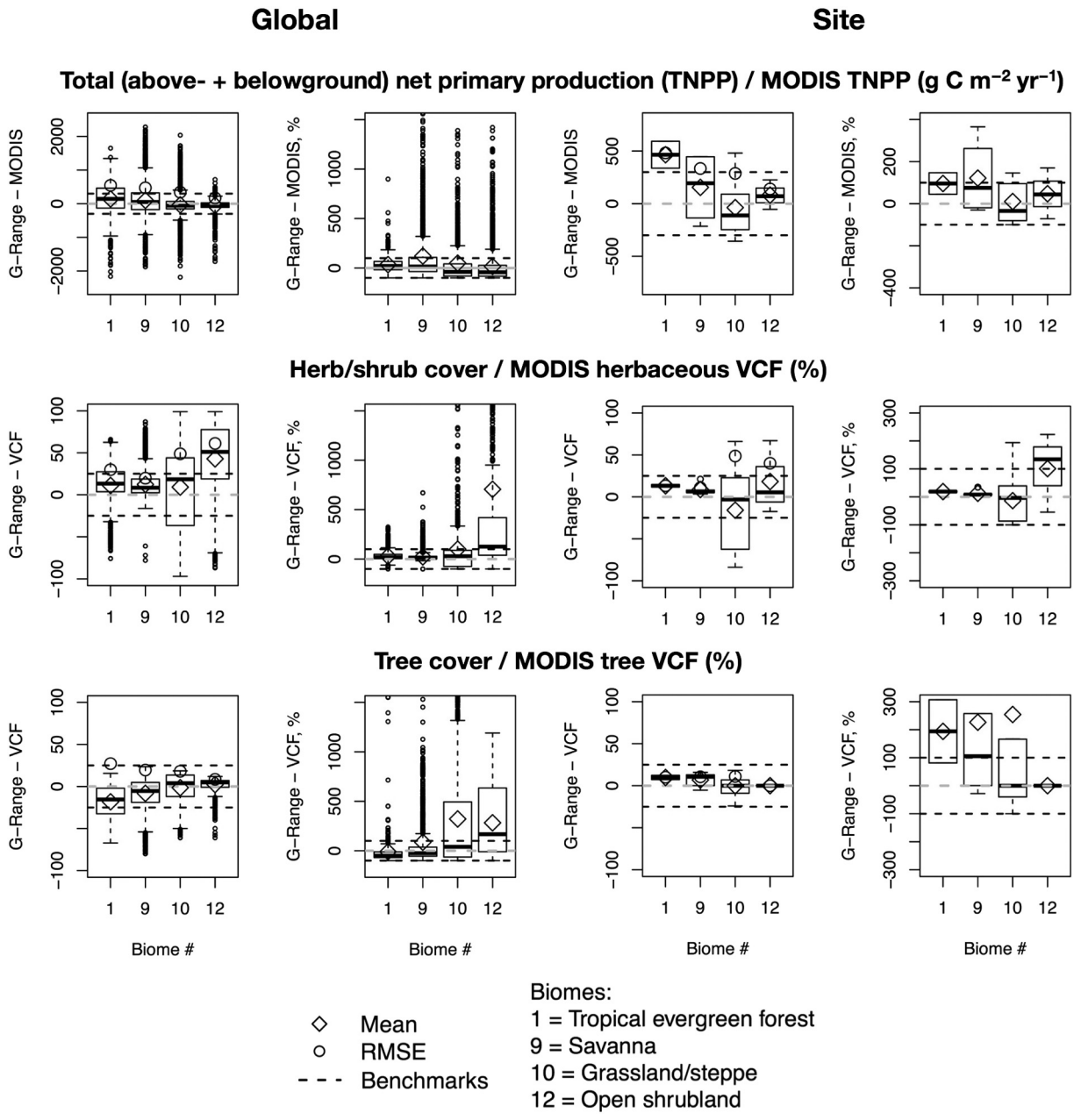

Figure 3. G-Range evaluation, on global and site scales, against global MODIS layers for annual total net primary production and fractional vegetation cover. Boxplots show the median and second and third quartiles, overlain with means, root mean squared error, and evaluation benchmarks.

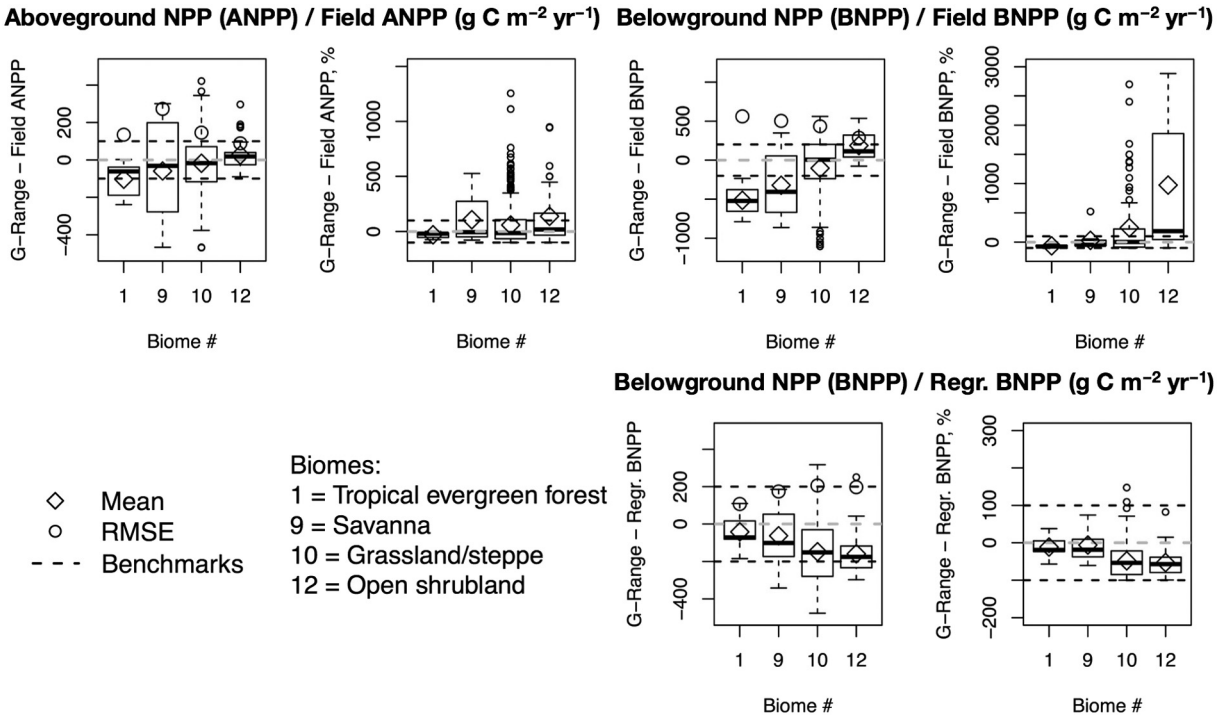

Figure 4. Site-scale G-Range evaluation against field measures of annual aboveground net primary production and annual belowground net primary production (BNPP) from field measures and global regression (regression BNPP). Boxplots show the median and second and third quartiles, overlain with means, root mean squared error, and evaluation benchmarks.

average within benchmarks for absolute, but not percent, difference from field BNPP. G-Range was always within benchmarks for regression BNPP.

Global difference in G-Range herb/shrub (facet) cover from MODIS VCF herbaceous cover was low for all biomes other than open shrubland (see Table 1, Fig. 3, Fig. E.2). At site scales, herb/shrub cover in open shrubland again exceeded the percent benchmark, although slightly.

Absolute difference in global G-Range tree (facet) cover from MODIS VCF tree cover was generally low, as was percent difference for those biomes with significant tree cover, tropical evergreen forest and savanna (see Table 1, Fig. 3, Fig. E.3). At site scales, tree cover in G-Range was comparable to MODIS VCF. Sites in all biomes other than open shrubland (which had no trees) exceeded the percent difference benchmark for tree cover.

All output variables met the established evaluation criteria in most of the focal biomes, as they were generally within one or both benchmarked differences from evaluation data at both scales of analysis. Unsurprisingly, biomes with higher values (e.g., more productive biomes) had a greater tendency to attain percent difference benchmarks, while biomes with lower values achieved absolute difference benchmarks more easily. Modest changes in parameter values and model errors with respect to the different NPP datasets revealed significant trade-offs precluding maximization of model fit to all evaluation datasets at all scales.

The sign of absolute difference in G-Range NPP from the MODIS and field NPP datasets exhibited consistent, opposing trends along the productivity gradient among biomes (see Table 1, Figs. 3 and 4). In more productive biomes, G-Range TNPP tended to exceed MODIS TNPP at both global and site scales and tended to be lower than MODIS in less productive biomes (see Table 1, Fig. 3). In contrast, G-Range NPP fell below field measures of ANPP and BNPP in more productive biomes, with errors trending positive as biome productivity decreased (see Table 1, Fig. 4). No such trade-off was apparent in grasslands, where NPP exhibited generally good, if somewhat conservative, fits to the MODIS and field datasets for NPP.

Vegetation cover was generally within benchmarks and indicative of similar vegetation composition to MODIS observations. There was one exception, that G-Range herb/shrub cover was substantially higher than MODIS herbaceous VCF in open shrubland. As during calibration, facet covers fluctuated around dynamic equilibria approximating MODIS VCF vegetation cover over the course of a 2 000-yr spin-up simulation. That is, facet covers did not surge or crash dramatically but rather shifted slowly and moderately in response to variation in climatic conditions and competition among vegetation facets, with little change in long-term means.

Superior fits to evaluation data were achievable, for each individual G-Range output variable, at each individual scale of assessment. However, further reductions in simultaneous divergence from multiple evaluation datasets and scales were constrained by trade-offs in model fit among variables, evaluation datasets, and scales. Changes to parameter settings that substantively improved model fit for any specific output either degraded model fit to other evaluation datasets or degraded fit at the other scale of analysis. That is, improving model fit for one specific variable, at one specific scale of analysis, invariably worsened model fit for other variables or scales. Moreover, variable- and scale-specific gains in model fit generally came at the cost of poorer fits to global calibration layers.

Discussion

Calibration of G-Range with global layers from CENTURY and other sources established initial confidence in the model (Boone et al., 2013), and evaluation provided further confirmation of the performance of G-Range given its structure, parameterization, and purpose. Evaluation of G-Range against multiple datasets from different sources and scales demonstrated the ability of the model to emulate important structural (cover) and functional (NPP) attributes of rangeland ecosystems in globally prominent rangeland biomes, as well as for sites within those biomes. The current G-Range implementation is appropriate for global-scale application (and, in some cases, at regional and national

scales), especially long-term simulation and projection of ecosystem processes, ecosystem services, and vegetation states in rangelands. For projections of rangeland ecosystem responses to climate change through 2050 using G-Range, see Boone et al. (2018).

Drawing the linkages between biogeochemistry and vegetation cover is advantageous in rangelands and drylands because ecosystem processes and services are known to vary with the dominance of different vegetation types (Anderies et al., 2002; Hibbard et al., 2003; Huxman et al., 2005). For example, an increase in fire frequency in a mixed herbaceous–woody system will typically cause the populations and cover of woody shrubs and trees to decline relative to grasses, causing rates of ecosystem processes at system level to increasingly reflect the rising dominance of herbaceous plants. Generally, a system-level shift toward grassy dominance would increase root-to-shoot ratio (Jackson et al., 2007) and proportional belowground carbon allocation and might reduce primary production and total ecosystem C storage (Eldridge et al., 2011). In arid systems, a grassy state can be more productive than shrubs (Knapp et al., 2008), resulting in positive feedbacks on ecosystem processes mediated by ecosystem productivity. Even where primary production and carbon storage decline under a grassy state, other ecosystem services may improve (Veldman et al., 2015), including hydrological flows (Jackson et al., 2005) and production of grass forage for grazing animals. The rationale for including bare ground in G-Range will be obvious to rangeland scientists, while global models that lack bare ground have limited applicability in rangelands.

The evaluation process identified overestimation and underestimation by G-Range in relation to various sources of evaluation data, with some errors contradicting one another. Each evaluation dataset has its own merits, and no unequivocally superior source of evaluation data exists for any output variable considered here, at global or site scales. Our approach was to harmonize model fit among multiple evaluation datasets from divergent origins and methodologies, each credible in the ecological and rangeland sciences. With each dataset contributing its version of "truth," this approach tests whether the current model implementation integrates across the information embedded in evaluation datasets from various sources, methodologies, and scales. Here, some evaluation datasets—belowground production (BNPP) and remotely sensed herbaceous cover (MODIS herbaceous VCF)—are considered in spite of their methodological limitations and higher uncertainty, as they play critical roles in rangeland ecosystems.

Belowground production has important implications for ecosystem services, such as soil improvement, C sequestration, and hydrological function, but it is known that BNPP is highly uncertain in perennial grasslands and other rangelands (see also Appendix E). Site-level model errors for field BNPP were to some extent attributable to the methods used to quantify root production under field conditions. BNPP estimated from regression (Gill et al., 2002), a questionable method—due to its reliance on turnover rates derived from sequential coring techniques known to be unreliable (Milchunas, 2009)—was presented for comparison with the techniques we prefer for quantifying BNPP. Root biomass coring methods can either underestimate or overestimate BNPP, depending on rates of root biomass turnover and yr-to-yr carryover of biomass largely associated with temperature. The likelihood of both underestimation and overestimation in different regions drove development of the approach for calculating BNPP from biomass harvests employed here (for full details, see Appendix E). BNPP from this "bracketing" method should be closer to "true" BNPP and had lower uncertainty (lower coefficient of variation) than alternative methods of estimating BNPP from biomass harvest, though its uncertainty remains high (Sircely, unpublished data).

MODIS NPP and herbaceous VCF products can have significant limitations in some regions, including drylands and the global tropics. In arid regions known to have significant herbaceous cover, the commonness of low or zero values (or incalculable; "no-data") for MODIS products may be partly attributable to satellite signal limitations (Zhao and Running, 2008), growth constraints in the MODIS GPP and NPP algorithms (Gebremichael and Barros, 2006; Mu et al., 2007), and the limited number of independent evaluation assessments conducted for herbaceous VCF. Because MODIS NPP and herbaceous VCF appear to frequently underestimate both NPP and herbaceous vegetation cover in arid systems, some apparent overestimation by G-Range with respect to MODIS-derived values for TNPP and herb and shrub cover may therefore be desirable in some areas known to have sparse but significant herbaceous cover (of course, these errors may be quite undesirable and problematic in truly barren rangelands). Although promising remote-sensing approaches for separating fractional cover of different vegetation types are in development (Guerschman and Hill, 2018), there are currently few alternatives to MODIS herbaceous VCF for evaluation of vegetation structure on a global scale. A particularly salient observation from evaluation was the presence of recalcitrant trade-offs in model fit among output variables (NPP vs. facet cover), evaluation data sources (MODIS vs. field), and spatial scales (global vs. site). Some trade-offs, especially for NPP, were unequivocally apparent in the sign of error (see Table 1), regardless of parameterization. Assuming that MODIS and field NPP contain equally valid information, these trends indicate a general trade-off facing model parameterization, precluding maximal model fit to both MODIS and field NPP. Other trade-offs were observed through parameter adjustments, notably surging or crashing of either NPP or the cover of a certain facet. The current model parameterization is not universally optimized, and computationally intensive permutation of parameter values to resolve comprehensive response surfaces would be valuable, though it is unclear how much accuracy would be gained.

The observed trade-offs in model fit suggest that multidimensional constraints limit the achievable external validity of simulations given available evaluation datasets. Such pervasive trade-offs suggest that dramatic changes to model parameterization would be warranted in the presence of more accurate evaluation data, over longer time scales, at greater spatial extents (for field data), or at finer spatial resolution (for remote sensing datasets). Though challenging for future improvement of the model, and for simulation of the global rangelands more generally, the observed trade-offs indicated that, to the extent feasible, the current model parameterization harmonized model fit across vastly different scales with respect to the selected evaluation datasets.

G-Range employs mechanistic representation of ecosystem processes grounded by largely phenomenological reproduction of historical vegetation structure. The ability of G-Range to reproduce observed historical vegetation structure (from MODIS VCF) over millennia-long simulations with limited divergence suggests that interactions among vegetation facets in the model may adequately represent the joint outcomes of the myriad, complex mechanisms through which real plants interact. For example, the effect of moisture stress (H_2O:PET) on establishment or death can be considered to reflect not only the combined effects of water and heat stress but also the multiple factors influencing complex interactions among water availability, temperature, and plant competition. The goal in developing the G-Range plant populations' submodels was to represent the joint outcomes of abiotic, management, and competitive effects on plant population dynamics, rather than specific effects of each factor.

In representing coupled changes in vegetation and ecosystem function, G-Range presents an alternative to other existing models, notably dynamic global vegetation models (DGVMs), which generally emphasize mechanism over phenomenological representation of empirical data or observations (e.g., Sitch et al., 2008; Piao et al., 2013). The calibration objective of dynamic G-Range facet covers diverging only modestly from historical vegetation cover (from MODIS VCF) following a 2 000-yr simulation stands in contrast to seeking mechanistic representation of vegetation interactions in globally distributed rangelands as diverse as savannas, semideserts, and humid tropical grasslands. In arid and semiarid rangelands, vegetation interactions and the relative effects of multiple ecosystem change drivers remain uncertain and vigorously

debated (D'Odorico et al., 2013), posing a significant challenge to mechanistic representation. In the global rangelands, it was deemed more pragmatic to collapse the wide variety of factors affecting plant establishment and death into a minimal set of parameters tuned to maintain long-term (2 000 yr) dynamic equilibria around historical vegetation patterns under 20th century climatic conditions.

Competition among facets leading to reduced establishment is represented explicitly in the plant populations' submodels, while any facilitation of establishment is implicit. The phenomenological training of the plant populations' submodels on MODIS VCF constrained parameter settings for facet interactions to negative values; parameterizing positive response curves is possible but can produce massive overestablishment (e.g., "deserts" with full grass cover). The assumption of a net-negative tendency for facet interactions is a simplification of actual plant interactions, which are a net of negative and positive effects. Interfacet competition for light, soil nutrients, or water follows CENTURY in assuming overstory suppression of understory production.

Net positive effects of woody plants on herbaceous production prevail at fine scales in arid and semiarid rangelands (Dohn et al., 2013), effects that could scale up to affect herbaceous establishment, mortality, and facet cover over large areas. However, in a semiarid savanna, competition between woody and herbaceous plants became more apparent as scale increased even within a single site (Riginos et al., 2009). Different plant growth forms, or functional types, generally have a competitive advantage under certain environmental conditions, meaning that woody-herbaceous competition could prevail over facilitation at greater scales. The net-negative assumption should be more valid over the large scales and multiple years for which G-Range is designed and is more likely to be violated in arid rangelands than in semiarid to humid rangelands.

In arid rangelands (e.g., < 200 mm yr^{-1}), climate and species composition could cause establishment to be effectively facilitation dependent (i.e., most establishment occurs under scattered woody canopies, in most years), thus violating the net negative assumption. Even in arid rangelands, facilitation in years of higher rainfall can give way to transient competition during drier years (Tielborger and Kadmon, 2000; Jankju, 2013), meaning that facilitation could boost establishment more strongly when it is less important (under "average" rainfall, establishment in arid rangelands is widespread and largely decoupled from plant interactions). Using variation in climatic conditions within desert and semidesert ("open shrubland" and "dense shrubland") biomes to modulate parameterized plant interactions (response curves) might improve model performance in dry rangelands. Where facilitation is not of overwhelming importance for establishment, the assumption of net negative facet interactions appears likely to hold.

The empirical training of the plant populations' submodels is the most important phenomenological element of the model, though not the only one. Another example is the effect of future atmospheric CO_2 levels on productivity; the Farquhar equation used in some DGVMs (e.g., LPJ; Ardö, 2015) prevents downregulation of photosynthesis at high CO_2 (El Maayar et al., 2006). G-Range, like CENTURY, takes the more phenomenological approach of scheduling CO_2 effects on productivity using input files. Further, and also unlike DGVMs, G-Range does not attempt mechanistic representation of biome distributions. While DGVMs allow for process-based migration of biomes in response to forcing drivers (especially climate), biome distributions are static in G-Range. Rather, gross vegetation composition—the balance among trees, shrubs, herbs, and bare ground—shifts within biomes in G-Range, resulting in potentially major changes in vegetation structural configuration, without altering biome distributions. Allowing vegetation structure and cover to shift within biomes, resulting in a hodgepodge of emergent configurations, may be more realistic than assuming migration of biome-specific vegetation. In preventing biomes from migrating, G-Range may produce more conservative (or more pessimistic) results where existing ecosystems are vulnerable to climate change, which comports with known limitations on species and ecosystem range shifts, such as dispersal and habitat fragmentation (Svenning and Sandel, 2013). By combining process-based (biogeochemistry) and empirical (vegetation dynamics) modeling approaches, G-Range forms part of the trend toward complementary integration of mechanism and phenomenology in ecosystem modeling (Adams et al., 2013).

The central advantage of G-Range is that it allows global change drivers to directly and independently modify ecosystem processes versus vegetation structure, as well as indirectly through interactions and feedbacks between ecosystem processes and vegetation dynamics. The effects of climate change can thus be predominately mediated by either climatic effects on ecosystem processes (e.g., diminished productivity due to drought) or climate-induced vegetation change (e.g., expansion of shrubs into former grasslands), and similarly, management drivers can force changes primarily through either biogeochemical or vegetation pathways.

The greatest sources of uncertainty in G-Range parameterization and performance are the relative effects of drivers such as climate, fire, grazing, and atmospheric CO_2 on vegetation change in rangelands. Furthermore, the current implementation of the plant populations' submodels responsible for vegetation change in G-Range is capable of producing multiple solutions. Replicated regional simulation experiments using G-Range to reproduce trends of vegetation change would help train the model to more precisely reflect specific or combinatory drivers of rangeland vegetation change. Because G-Range can emulate vegetation structure under historical climatic conditions over the course of 2 000-yr simulations, major divergences from historical vegetation patterns driven by climate and CO_2 scenarios should primarily indicate climate and CO_2 effects rather than model specification. Still, G-Range should be applied across a range of climate and CO_2 scenarios to address uncertainty in climatic input datasets.

In light of the model evaluation results, the structure and parameterization of G-Range can be deemed sufficient for a variety of uses. Appropriate applications of the current model configuration include simulating and forecasting the cycling of C, N, and water, as well as vegetation states and their dynamics, in rangeland ecosystems on a global scale. While G-Range can be applied at regional or even national scales, spatial variation in model performance should be assessed before model application. G-Range is particularly well suited to generating medium- (e.g., decadal) to long-term projections of the impacts of changes in climate and atmospheric CO_2 on ecosystem services, such as forage and browse production and C sequestration. Such forecasts can help gauge the long-term production potential of existing rangeland systems given future climatic and atmospheric conditions and provide guidance where novel drylands develop as a result of aridification. Forecasting the future structure and function of rangeland ecosystems can provide a foundation for developing and targeting feasible options for adapting rangeland systems to withstand changes in climate and atmospheric CO_2 and mitigating CO_2 emissions in rangelands and other drylands.

Supplementary data to this article can be found online at https://doi.org/10.1016/j.rama.2019.03.002.

References

Adams, H., Williams, A., Xu, C., Rauscher, S., Jiang, X., McDowell, N., 2013. Empirical and process-based approaches to climate-induced forest mortality models. Frontiers in Plant Science 4, 1–5.

Anderies, J.M., Janssen, M.A., Walker, B.H., 2002. Grazing management, resilience, and the dynamics of a fire-driven rangeland system. Ecosystems 5, 23–44.

Ardö, J., 2015. Comparison between remote sensing and a dynamic vegetation model for estimating terrestrial primary production of Africa. Carbon Balance Management 10, 8.

Armstrong, R., Brodzik, M.J., Knowles, K., Savoie, M., 2005. Global monthly EASE-Grid snow water equivalent climatology: snow water equivalent.Available at:. http://nsidc.org/data/docs/daac/nsidc0271_ease_grid_swe_climatology.gd.html Accessed 22 April 2011.

Batjes, N.H., 2002. Revised soil parameter estimates for the soil types of the world. Soil Use Management 18, 232–235.

Boone, R.B., Conant, R.T., Hilinski, T.E., 2011. G-Range: development and use of a beta global rangeland model. CGIAR Research Program on Climate Change, Agriculture

and Food Security (CCAFS) and International Livestock Research Institute (ILRI), Nairobi Kenya.
Boone, R.B., Conant, R.T., Sircely, J., 2013. Adjustment and sensitivity analyses of a beta global rangeland model. CGIAR Research Program on Climate Change, Agriculture and Food Security (CCAFS) and International Livestock Research Institute (ILRI), Nairobi Kenya.
Boone, R.B., Conant, R.T., Sircely, J., Thornton, P.K., Herrero, M., 2018. Climate change impacts on selected global rangeland ecosystem services. Global Changes in Biology 24, 1382–1393.
Coughenour, M.B., 1994. Savanna landscape and regional ecosystem model—model description Natural Resource Ecology Laboratory (NREL), Colorado State University, Fort Collins, CO, USA.
Cramer, W., Bondeau, A., Woodward, F.I.A.N., Prentice, I.C., Betts, R.A., Brovkin, V., Cox, P.M., Fisher, V., Foley, J.A., Friend, A.D., Kucharik, C., Lomas, M.R., Ramankutty, N., Sitch, S., Smith, B., 2001. Global response of terrestrial ecosystem structure and function to CO_2 and climate change: results from six dynamic global vegetation models. Global Changes in Biology 7, 357–373.
CRU, 2008. CRU Time Series (TS) 3.0 high resolution gridded datasets East Anglia, UK.
D'Odorico, P., Bhattachan, A., Davis, K.F., Ravi, S., Runyan, C.W., 2013. Global desertification: drivers and feedbacks. Advances in Water Resources 51, 326–344.
Dardel, C., Kergoat, L., Hiernaux, P., Mougin, E., Grippa, M., Tucker, C.J., 2014. Re-greening Sahel: 30 years of remote sensing data and field observations (Mali, Niger). Remote Sensing in the Environment 140, 350–364.
Derner, J.D., Augustine, D.J., Ascough, J.C., Ahuja, L.R., Derner, J.D., Augustine, D.J., Ii, J.C.A., Ahuja, L.R., 2012. Opportunities for increasing utility of models for rangeland management. Rangeland Ecology & Management 65, 623–631.
Dohn, J., Dembélé, F., Karembé, M., Moustakas, A., Amévor, K.A., Hanan, N.P., 2013. Tree effects on grass growth in savannas: competition, facilitation and the stress-gradient hypothesis. Journal of Ecology 101, 202–209.
El Maayar, M., Ramankutty, N., Kucharik, C.J., 2006. Modeling global and regional net primary production under elevated atmospheric CO_2: on a potential source of uncertainty. Earth Interactions 10, 1–20.
Eldridge, D.J., Bowker, M.A., Maestre, F.T., Roger, E., Reynolds, J.F., Whitford, W.G., 2011. Impacts of shrub encroachment on ecosystem structure and functioning: towards a global synthesis. Ecology Letters 14, 709–722.
GASL, 2014. Towards sustainable livestock—global agenda for sustainable livestock. GASL, Rome, Italy, p. 14.
Gebremichael, M., Barros, A.P., 2006. Evaluation of MODIS Gross Primary Productivity (GPP) in tropical monsoon regions. Remote Sensing in the Environment 100, 150–166.
Gill, R.A., Kelly, R.H., Parton, W.J., Day, K.A., Jackson, R.B., Morgan, J.A., Scurlock, J.M.O., Tieszen, L.L., Castle, J.V., Ojima, D.S., Zhang, X.S., 2002. Using simple environmental variables to estimate below-ground productivity in grasslands. Global Ecology Biogeography 11, 79–86.
Grice, A.C., Hodgkinson, K.C., 2002. Challenges for rangeland people. In: Grice, A.C., Hodgkinson, K.C. (Eds.), Global rangelands: progress and prospects. CAB International, New York, NY, USA.
Guerschman, J.P., Hill, M.J., 2018. Calibration and validation of the Australian fractional cover product for MODIS collection 6. Remote Sensing Letters 9, 696–705.
Hansen, M., DeFries, R.S., Townshend, J.R.G., Carroll, M., Dimiceli, C., Sohlberg, R.A., 2006. Vegetation Continuous Fields MOD44B, Collection. University of Maryland, College Park, MD, USA.
Henderson, B.B., Gerber, P.J., Hilinski, T.E., Falcucci, A., Ojima, D.S., Salvatore, M., Conant, R.T., 2015. Greenhouse gas mitigation potential of the world's grazing lands: modeling soil carbon and nitrogen fluxes of mitigation practices. Agricultural Ecosystems and the Environment 207, 91–100.
Hibbard, K.A., Schimel, D.S., Archer, S., Ojima, D.S., Parton, W., 2003. Grassland to woodland transitions: integrating changes in landscape structure and biogeochemistry. Ecology Applications 13, 911–926.
Huxman, T.E., Wilcox, B.P., Breshears, D.D., Scott, R.L., Snyder, K.A., Small, E.E., Hultine, K.R., Pockman, W.T., Jackson, R.B., 2005. Ecohydrological implications of woody plant encroachment. Ecology 86, 308–319.
Jackson, R., Jobbagy, E., Avissar, R., Roy, S., Barrett, D., Cook, C., Farley, K., le Maitre, D., McCarl, B., Murray, B., 2005. Trading water for carbon with biological sequestration. Science 80:310, 1944–1947.
Jackson, R., Farley, K., Hoffmann, W., Jobbágy, E., McCulley, R., 2007. Carbon and water tradeoffs in conversions to forests and shrublands. In: Canadell, J., Pataki, D., Pitelka, L. (Eds.), Terrestrial ecosystems in a changing world. Springer, Berlin, Germany, pp. 237–246.
Jankju, M., 2013. Role of nurse shrubs in restoration of an arid rangeland: effects of microclimate on grass establishment. Journal of Arid Environments 89, 103–109.
Knapp, A., Briggs, J., Collins, S., Archer, S., Bret-Harte, M., Ewers, B., Peters, D., Young, D., Shaver, G., Pendall, E., Cleary, M., 2008. Shrub encroachment in North American grasslands: shifts in growth form dominance rapidly alters control of ecosystem carbon inputs. Global Changes in Biology 14, 615–623.
Le Houérou, H.N., Bingham, R.L., Skerbek, W., 1988. Relationship between the variability of primary production and the variability of annual precipitation in world arid lands. Journal of Arid Environments 15, 1–18.
Milchunas, D.G., 2009. Estimating root production: comparison of 11 methods in shortgrass steppe and review of biases. Ecosystems 12, 1381–1402.
Mu, Q., Zhao, M., Heinsch, F.A., Liu, M., Tian, H., Running, S.W., 2007. Evaluating water stress controls on primary production in biogeochemical and remote sensing based models. Journal of Geophysical Research 112, G01012.
NREL, 2000. Century Homepage [WWW Document]. Nat. Resour. Ecol. Lab. (NREL), Color. State Univ. URL. https://www2.nrel.colostate.edu/projects/century/.
NREL, 2012. CENTURY Publications [WWW Document]. Nat. Resour. Ecol. Lab. (NREL), Color. State Univ. URL. https://www2.nrel.colostate.edu/projects/century-publications.html.
NREL, 2013. G-Range homepage. Natural Resources Ecology Laboratory, color. State University.Available at:. http://www2.nrel.colostate.edu/projects/grange/ Accessed 13 June 2018.
Parton, W.J., Schimel, D.S., Cole, C.V., Ojima, D.S., 1987. Analysis of factors controlling soil organic matter levels in Great Plains grasslands. Soil Science Society of America Journal 51, 1173–1179.
Parton, W.J., Scurlock, J.M.O., Ojima, D.S., Gilmanov, T.G., Scholes, R.J., Schimel, D.S., Kirchner, T., Menaut, J.-C., Seastedt, T., Garcia-Moya, E., Kamnalrut, A., Kinyamario, J.I., 1993. Observations and modeling of biomass and soil organic matter dynamics for the grassland biome worldwide. Global Biogeochemical Cycles 7, 785–809.
Piao, S., Sitch, S., Ciais, P., Friedlingstein, P., Cong, N.A.N., Huntingford, C., Jung, M., 2013. Evaluation of terrestrial carbon cycle models for their response to climate variability and to CO_2 trends. Global Changes in Biology 19, 2117–2132.
Ramankutty, N., Foley, J., 1999. Estimating historical changes in global land cover: croplands from 1700 to 1992. Global Biogeochemical Cycles 13, 997–1027.
Reid, R.S., Fernández-Giménez, M.E., Galvin, K.A., 2014. Dynamics and resilience of rangelands and pastoral peoples around the globe. Annual Review in Environmental Resources 39, 217–242.
Reynolds, J.F., Smith, D., Stafford, M., Lambin II, E.F., Turner, B.L., Mortimore, M., Batterbury, S.P.J., Downing, T.E., Dowlatabadi, H., Fernández, R.J., Herrick, J.E., Huber-sannwald, E., Jiang, H., 2007. Global desertification: building a science for dryland development. Science 316, 847–851.
Riginos, C., Grace, J.B., Augustine, D.J., Young, T.P., 2009. Local versus landscape-scale effects of savanna trees on grasses. Journal of Ecology 97, 1337–1345.
Ruesch, A., Gibbs, H.K., 2008. New IPCC tier-1 global biomass carbon map for the year 2000.Available at:. http://cdiac.ornl.gov Accessed 22 April 2011.
Scurlock, J.M.O., Johnson, K., Olson, R.J., 2002. Estimating net primary productivity from grassland biomass dynamics measurements. Global Changes in Biology 8, 736–753.
Sietse, O.L., 2010. ISLSCP II FASIR-adjusted NDVI Biophysical Parameter Fields, 1982-1998. Available at:. http://daac.ornl.gov/ Accessed 22 April 2011.
Sitch, S., Huntingford, C., Gedney, N., Levy, P.E., Lomas, M., Piao, S.L., Betts, R., Ciais, P., Cox, P., Friedlingstein, P., Jones, C.D., Prentice, I.C., Woodward, F.I., 2008. Evaluation of the terrestrial carbon cycle, future plant geography and climate-carbon cycle feedbacks using five Dynamic Global Vegetation Models (DGVMs). Global Changes in Biology 14, 2015–2039.
Svenning, J.-C., Sandel, B., 2013. Disequilibrium vegetation dynamics under future climate change. American Journal of Botany 100, 1266–1286.
Tielborger, K., Kadmon, R., 2000. Temporal environmental variation tips the balance between facilitation and interference in desert plants. Ecology 81, 1544–1553.
USGS, 2008. Global land cover characterization, version 2. Available at:. http://edc2.usgs.gov/glcc/glcc.php.
Veldman, J.W., Overbeck, G.E., Negreiros, D., Mahy, G., Stradic, S.L.E., 2015. Where tree planting and forest expansion are bad for biodiversity and ecosystem services. Bioscience 65, 1011–1018.
Von Wehrden, H., Hanspach, J., Kaczensky, P., Ficher, J., Weche, K., 2012. Global assessment of the non-equilibrium concept in rangelands. Ecology Applications 22, 393–399.
White, R.P., Tunstall, D., Henninger, N., 2002. An ecosystem approach to drylands: building support for new development policies. World Resources Institute (WRI), Washington, DC, USA, pp. 14.
Zhang, K., Kimball, J.S., Nemani, R.R., Running, S.W., 2010. A continuous satellite-derived global record of land surface evapotranspiration from 1983 to 2006. Water Resource Research 46, W09522.
Zhao, M., Running, S.W., 2008. Remote sensing of terrestrial primary production and carbon cycle. In: Liang, S. (Ed.), Advances in land remote sensing. Springer, College Park, MD, USA, pp. 423–444.